Early Pleistocene stratigraphy, sedimentary environments, and formation contexts at Dmanisi in the Georgian Caucasus

Reid Ferring, Oriol Oms, Sebastien Nomade, John Humphrey, Martha Tappen, Reed Coil, Teona Shelia, Peter Crislip, Rusudan Chagelishvili, Gocha Kiladze, et al.

Early Pleistocene stratigraphy, sedimentary environments, and formation contexts at Dmanisi in the Georgian Caucasus

Reid Ferring [a, *], Oriol Oms [b], Sebastien Nomade [c], John D. Humphrey [d], Martha Tappen [e], Reed Coil [f], Teona Shelia [g], Peter Crislip [a], Rusudan Chagelishvili [g], Gocha Kiladze [g], Hervé Guillou [c], David Lordkipanidze [g]

[a] *Department of Geography and the Environment, 1155 Union Circle, University of North Texas, Denton, TX 76208, USA*
[b] *Department of Geology, Universitat Autònoma de Barcelona, 08193 Bellaterra, Spain*
[c] *Laboratoire des Sciences du Climat et de l'Environment LSCE/IPSL, UMR CEA-CNRS-UVSQ 8212 et Université Paris-Saclay, CEA Saclay, Bat 714, Orme des Merisiers, 91191 Gif sur Yvette, France*
[d] *Department of Geosciences, King Fahd University of Petroleum and Minerals, Dhahran 31261, Saudi Arabia*
[e] *Department of Anthropology, University of Minnesota, 395 Humphrey Center, 301 19th Ave. South, Minneapolis, MN 55755, USA*
[f] *Department of Sociology and Anthropology, Nazarbayev University, 53 Kabanbay Batyr Ave, Nur-Sultan 010000, Kazakhstan*
[g] *Georgian National Museum, 3/10 Shota Rustaveli Avenue, Tbilisi 0105, Georgia*

The Early Pleistocene site of Dmanisi is now well known for its large number of fossils of early *Homo erectus* as well as associated artifacts and faunal remains, recovered mainly in pipe-related geologic features. Testing in the M5 unit 100 m to the west of the main excavations revealed a thick stratigraphy with no evidence of pipes or gullies, indicating that the geologic record at Dmanisi included spatially distinct sedimentary environments that needed further investigation. Here we report the results of a geoarchaeological program to collect data bearing on contexts and formation processes over a large area of the promontory. That work has defined over 40,000 m^2 of in situ deposits with artifacts and faunas. Stratum A ashes bury the uppermost Mashavera Basalt, which we have dated to 1.8 Ma in the M5 block. The Stratum A deposits contain stratified occupations that accumulated quickly and offer good potential for recovery of in situ materials. Stratum B1 deposits above the A/B unconformity include all of the pipe and gully facies at Dmanisi, reflecting a brief but very intense phase of geomorphic change. Those de-posits contain the majority of faunas and all of the hominin fossils. B1 slope facies offer excellent for-mation contexts away from the piped area, and all B1 deposits are sealed by Stratum B2 over the whole promontory. Strata B2 to B5 register a return to slope facies, with no further evidence of pipes or gullies. Those deposits also present excellent contexts for recovery of in situ occupations. Overall, Dmanisi's geologic history preserves an exceptional record of the activities and environmental context of occu-pations during the first colonization of Eurasia.

1. Introduction

The ruins of the Medieval city of Dmanisi occupy the promontory at the confluence of the Mashavera and Pinezauri rivers in the lower Caucasus of southern Georgia (Fig. 1). A substantial settlement from the Bronze Age until the late Medieval Period, the entire surface of the promontory is covered by remains of masonry architecture, and a castle and fortress on the bedrock rise on the southern promontory (Fig. 1). Fortified by 80 m cliffs on two sides, and situated on the ancient silk road from the south, this was an ideal location for the ancient city. Remarkably, stratified Early Pleistocene deposits are preserved under the city ruins. Those deposits preserve thousands of animal fossils, lithic artifacts, and almost 80 fossils of early *Homo erectus* (Coil et al., 2020; Ferring et al., 2011; Gabunia and Vekua, 1995; Gabunia et al., 2000; Lordkipanidze et al., 2005, 2007, 2013; Margvelashvili et al., 2022; Mgeladze et al., 2011; Shelia et al., 2020; Vekua et al., 2002, 2005). Most of the recovered fossils and artifacts were from excavation Blocks 1 and 2 in the center of the Dmanisi promontory and were found in pipe and gully deposits of Stratum B1 (Fig. 1c).

From the first discoveries of Early Pleistocene fossils through the recovery of large samples of fossils in Blocks 1 and 2, it was clear that

* Corresponding author.
E-mail address: c.reid.ferring@unt.edu (R. Ferring).

bone preservation in these deposits was excellent (Tappen et al., 2002, 2007; Tappen 2009). The association of many lithic artifacts with those bones, and also numerous carnivore remains and carnivore-modified bones gave rise to obvious questions about agents of bone accumulation; importantly, geologic, taphonomic, and spatial analyses virtually excluded any possible role of fluvial processes in bone accumulation (Coil et al., 2020; Lordkipanidze et al., 2007; Tappen 2009). Rather, burial of bones in pipe and gully deposits did point to the important role of rapid sedimentation and weak weathering regimes in bone preservation (Coil et al., 2020; Ferring et al., 2011). While excavation and recovery of many fossils and artifacts continued in Block 2, the surrounding areas of the promontory were unknown, save for shallow exposures in tests done in the early 1990s (Djaparidze et al., 1989).

As excavations in Block 2 continued, test excavations were conducted over several seasons at M5, located about 100 m upslope from the main excavations in Block 2 (Fig. 1). The 6 m thick M5 section has nine conformably superposed stratigraphic units (Ferring et al., 2011) including a slope facies of Stratum B1 that contrasts with the B1 pipe and gully deposits in Blocks 1 and 2. The striking differences in the geology of M5, as well as the first discovery of artifacts in Stratum A deposits there, showed that Dmanisi's geoarchaeological record was spatially and stratigraphically extensive. Many more geoarchaeological exposures over the promontory were clearly necessary, and a program of testing was implemented. The goals of those studies were to better document the stratigraphic and spatial extent of archaeological and paleontological materials, recover data on the sedimentary and geomorphic contexts across the promontory, and continue efforts to better define the relative age ranges of the serially deposited strata.

Here we present a summary of the geoarchaeological investigations conducted in concert with expanded block and test excavations over the past eight field seasons (Figs. 1 and 2). These have provided substantial new data on the spatial extent, sedimentary environments, and formation contexts on the Dmanisi promontory. In addition, work at M5 includes dating the first sample of the Mashavera Basalt from the uppermost flows on the promontory surface, and petrographic study of the M5 section.

1.1. Background

The archaeological site of Dmanisi (41° 20′14.09″ N; 44° 20′ 41.66″) is located about 65 km southwest of the capital city of Tbilisi in the Kvemo Kartli region of Georgia (Fig. 1). The site is situated at an average elevation of 910 m mean sea level (msl) on a promontory that is formed on two sides by the deeply entrenched Mashavera and Pinezauri rivers (Fig. 1). The southwestern extremity of this promontory connects with upland hills (up to ca. 1200 m msl) that have formed on faulted Upper Cretaceous tuffs and ignimbrites. Higher hills (to ca. 1500 m msl) to the south formed on diverse plutonic, volcanic, metamorphic, and sedimentary rocks (Supplementary Online Material [SOM] Fig. S1). The diverse lithology of those rocks is represented in the modern Pinezauri River gravels as well as among the diverse raw materials of Dmanisi's lithic artifact assemblages (Baena et al., 2010; Ferring et al., 2011; Gudjabidze, 2003; Mgeladze et al., 2011).

There is no evidence that either of the rivers flowed across the sloping surface formed by the Mashavera Basalt. Accordingly, the paleohydrology of the promontory was that of slope in a small catchment basin on which eolian sediments were serially deposited and variably affected by weathering and colluvial processes.

Since the last Mashavera lava flows, Dmanisi has been a promontory standing above the confluence of the two rivers. Today those gorges are deeply incised, with vertical walls exposing up to 80 m of

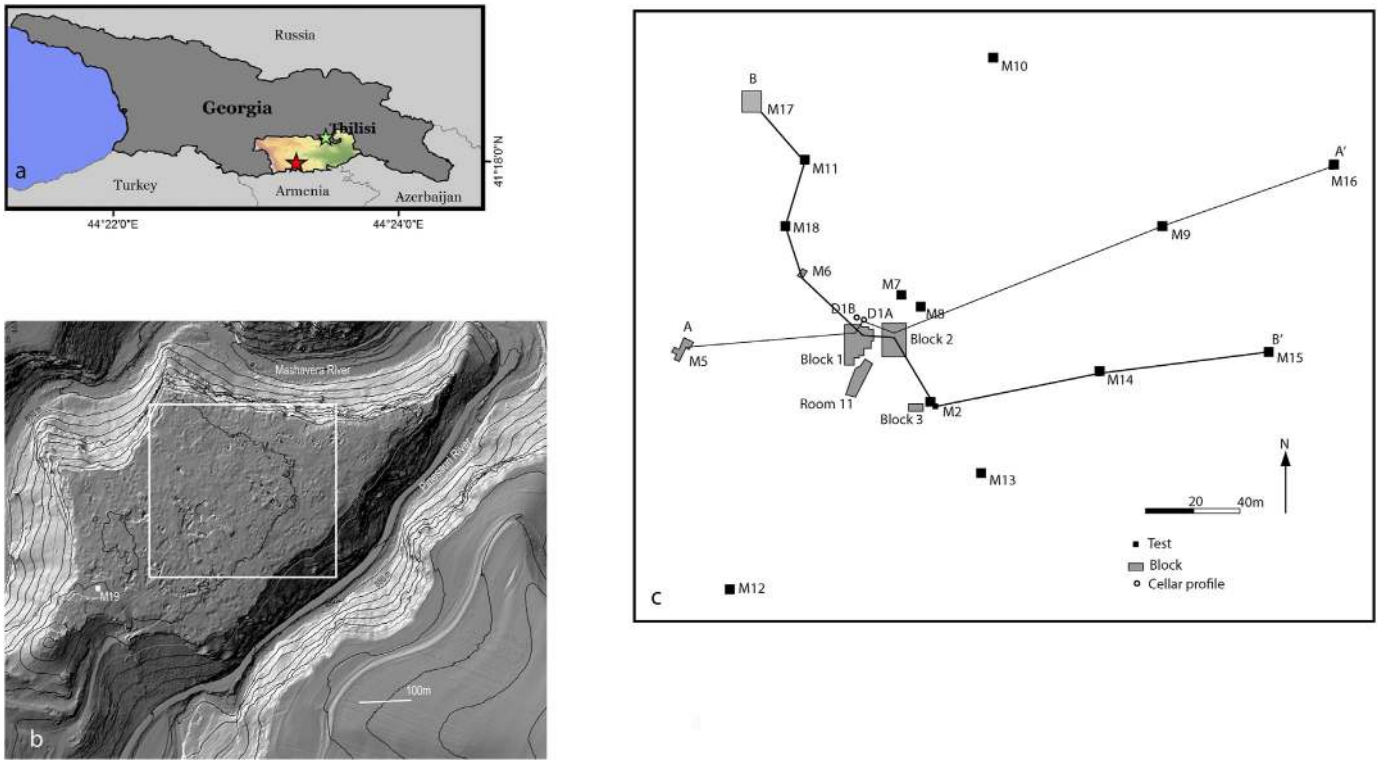

Figure 1. Location map and excavation areas on the Dmanisi promontory. a) Dmanisi is at about 910 m msl in the foothills of the lower Caucasus range. b) The Dmanisi promontory was formed by incision of the Mashavera and Pinesauri rivers after the Mashavera lava flows covered the bedrock spur at their confluence. Note profile M19, with sterile Stratum A ashes resting on Cretaceous bedrock, exposed under the Dmanisi church. Image provided by Laserscan Berlin. c) Block excavations and 1 m^2 test excavations show that Dmanisi preserves up to 6 m of stratified deposits with artifacts and faunal remains over an area of at least 40,000 m^2. Units M10, M13, and M16 did not have Dmanisi Formation sediments.

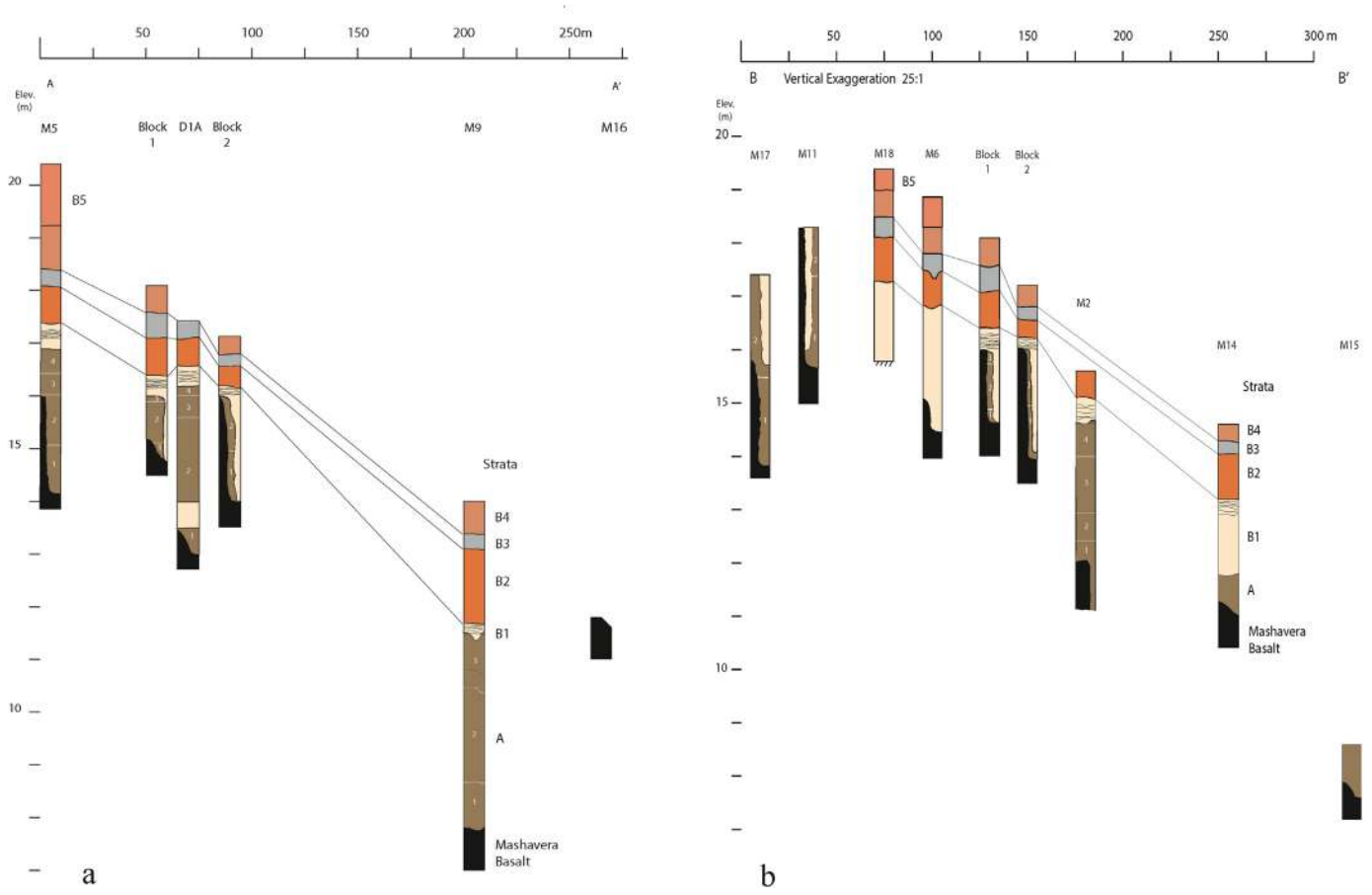

Figure 2. Stratigraphic cross sections on the Dmanisi promontory. All profiles in and to the left of Block 2 are on the upper promontory, where all pipe and gully facies are located. The steep drop to the lower promontory was controlled by the relief of the basalt. Note the stratigraphic correlations of strata B2 and higher, burying the B1 deposits across the whole promontory. See Figure 1 for locations of sections. Abbreviation: Elev. = elevation.

Mashavera Basalt that filled the gorge and covered the Cretaceous rocks forming the pre-Mashavera bedrock spur at the rivers' confluence (SOM Figs. S2 and S3). Exposures of the contact of the Mashavera Basalt with underlying rocks and sediments show that at the time of the lava flows, the steep-walled river valleys were nearly in their present positions, and that the surrounding upland landforms were probably quite similar to those of today (SOM Fig. S2). The Mashavera Valley is narrow and deep for ca. 20 km downstream from the promontory, where it opens to gentler slopes and broad alluvial terraces. West of the promontory, the Mashavera Valley rises rather steeply to an open plateau with elevations of ca. 2000 m near Dmanisi Town and continues to rise toward the Djavakheti ridge about 80 km from the site (Nomade et al., 2016).

1.2. Stratigraphy

Since the discovery of Early Pleistocene fossils at Dmanisi in 1983, two different stratigraphic schemes have been used. The first stratigraphic scheme recognized six subhorizontal strata (labeled I–VI) exposed in the 'Room 11' paleontological excavations and the early excavations in Block 1 (Fig. 1; Djaparidze et al., 1989; Jöris, 2008). A different scheme identified two major stratigraphic units (A and B) based on the unconformity at the A–B contact observed in profiles in and around Block 1, as well as piping features that formed in A strata but were filled with B sediments (Gabunia et al., 2000). The M5 section resolved uncertainties created by the complex stratigraphy of Blocks 1 and 2 and resulted in a formal stratigraphy for the Dmanisi Formation, composed of Stratum A (A1–A4) and Stratum B (B1–B5; Ferring et al., 2011). Expanded excavations as well as a testing program over the promontory, described later, have all showed that the A1–B5 stratigraphy of M5 is applicable to at least 40,000 m^2 of the promontory.

1.3. Piping: geologic background

The presence of pipe features at Dmanisi was first recognized in Block 1, Room 11, and the Medieval cellar profile (D1B) north of Block I by Ferring and Swisher (Fig. 1; Gabunia et al., 2000) who noted their implications for both stratigraphy and formation processes. Subsequent exposure of pipes and related gully features in Block 2 showed that those deposits contained all of the hominin fossils and the vast majority of vertebrate fossils from that block (Coil et al., 2020; Lordkipanidze et al., 2007, 2013). Clearly, piping and related gullying processes were key to understanding not only the sedimentary and geomorphic development of Dmanisi during the formation of Stratum B1 but also had to be evaluated as a possible factor in the accumulation of so many well-preserved bones.

Pipes are tunnel-like features that form on hillslopes and in gullies through the combined action of hydraulic erosion and mass movement within the pipes (Bernatek-Jakiel et al., 2017; Bryan and Jones, 1997; Farifteh and Soeters, 1999; Gutierrez et al., 1997; Halliday, 2007; Jones et al., 1997; Pickford, 2018; Verachtert et al., 2010, 2013; Zhu, 1997, 2012). Bernatek-Jakiel and Poesen's (2018)

comprehensive review shows that pipes have a truly global distribution, and exhibit remarkable variability with respect to climate, soil types, topographic settings as well as size, shape, and formation patterns. Pipe features at Dmanisi are all buried by Strata B2−B5, and are filled with B1 deposits. These 'paleopipe' features (see Saunders and Dawson, 1998), discussed later, include filled pipes, pipe breaches, and gullies formed on collapsed pipes.

1.4. Radiometric dating

Several attempts have been made since the early 2000s to date at the Dmanisi site (see SOM S1 and S2). All $^{40}Ar/^{39}Ar$ ages made directly on the Mashavera Basalt at Dmanisi and both the Mashavera and the Orzomani Basalts 14 km west of Dmanisi demonstrate that the Dmanisi formation is bracketed between 1.848 ± 0.008 Ma and 1.759 ± 0.005 Ma (2σ level; Gabunia et al., 2000; Messager et al., 2011; Nomade et al., 2016). The $^{40}Ar/^{39}Ar$ age of 1.81 ± 0.03 Ma and 1.81 ± 0.05 Ma obtained on stratum A1 ash by Garcia et al. (2010) and De Lumley and Lordkipanidze (2006), respectively, need to be taken with caution as they are based on very unprecise low K-bearing minerals (i.e., plagioclase) as well as glass shards that are known to be affected by ^{39}Ar recoil during irradiation and argon lost during alteration which can bias $^{40}Ar/^{39}Ar$ toward older ages. Accordingly, those ages will not be used hereafter. Unspiked K/Ar and $^{40}Ar/^{39}Ar$ have been obtained at the LSCE Laboratory (France). Detailed methodological and analytical protocols for each method can be found in SOM S1.

1.5. Paleomagnetic dating

All previous paleomagnetic studies were carried out in the thin lithological sections from Blocks 1 and 2, where piping and gulling is the rule rather than the exception (see SOM S2). This scenario was completely different when the M5 section was studied by Ferring et al. (2011). This vertically ordered section (free of gullies and pipes) was thicker (6 m) and displayed a clear paleomagnetism. Again, normal (Olduvai) and reverse (upper Matuyama) polarities were recorded in A and B strata, respectively.

2. Materials and methods

2.1. Stratigraphy, sediment-soils analysis

Sediment-soils investigations were conducted on profiles of block excavations, test units, and also profiles exposed by excavation of Medieval cellars D1B and M19 (Fig. 1c). Profiles around Block 1 were also afforded by foundation excavations (M7, M8). All profiles were described and sampled with procedures in Ferring et al. (2011). Textural and carbonate analyses were conducted for the M5 and M9 profiles (Gee and Bauder, 1986). Petrographic analysis of 15 thin sections from M5 followed standard procedures (Stoopes, 2003), and also included scanning electron microscopy (SEM) and energy dispersive spectroscopy (EDS) for mineralogy and geochemistry (Crislip, 2013). See also SOM S2.

2.2. K/Ar and $^{40}Ar/^{39}Ar$ dating

A single hand sample (about 500 g) was extracted from the collapsed basalt slab in direct contact with stratum A in the M5 Block to be dated by unspiked K/Ar and $^{40}Ar/^{39}Ar$ techniques. The fresh cut displayed a homogenous dark blue and shiny microlithic texture, with well-preserved phenocrysts of olivine as well as pristine plagioclase. Groundmass from this sample was prepared following the methods described in Guillou et al. (1998). Aliquots from the same separates were used for both unspiked K/Ar and $^{40}Ar/^{39}Ar$ age determinations. Phenocrysts and xenocrysts, which are potential carriers of extraneous ^{40}Ar (including excess and inherited components), were eliminated using magnetic, gravimetric, and visual hand-picking separation. The unspiked K/Ar technique and the $^{40}Ar/^{39}Ar$ method are detailed in SOM S1.

2.3. Paleomagnetism

In the present work, we introduce the magnetostratigraphic results from the M6 and M11 sections, reported for the first time. Laboratory demagnetization of samples was mainly carried out on a 2G triaxial cryogenic magnetometer at the Paleomagnetism Laboratory at (GEO3BCN-CSIC CCIT-Universitat de Barcelona). Samples underwent a stepwise thermal demagnetization from room temperature to up to 550 °C and susceptibility measures were taken during the whole process in order to detect the eventual formation of magnetic minerals (see detailed procedures in Ferring et al., 2011).

3. Results

3.1. Unspiked K/Ar and $^{40}Ar/^{39}Ar$ results

Four distinct measurements of ^{40}Ar made on pure groundmass allowed us to calculate four unspiked K/Ar ages ranging from 1.77 ± 0.04 and 1.79 ± 0.05 Ma (2σ level; SOM Table S1).

The two $^{40}Ar/^{39}Ar$ heating experiments provided spectra including 100% of the extracted gas defining the age plateaus (SOM Fig. S4). The two plateau ages (i.e., 1.815 ± 0.029 Ma and 1.811 ± 0.024 Ma; 2σ level) are indistinguishable within uncertainty allowing us to calculate a combined age of 1.813 ± 0.022 Ma (2σ level; SOM Fig. S4a). The inverse isochron diagram built using the two independent experiments does not evidence apparent excess argon (SOM Fig. S4b). Because of the limited spreading along the inverse isochron the age is less precise than the plateau ages. Therefore, we retain the combined plateau age (i.e., 1.813 ± 0.022 Ma) as the final $^{40}Ar/^{39}Ar$ age.

Because the $^{40}Ar/^{39}Ar$ ages and the K/Ar ages are equivalent at the 2σ level confidence, we feel confident to pool all 6 ages together to calculate a more precise and robust age of 1.799 ± 0.014 Ma (2σ level) for the eruption which delivered the Mashavera Basalt in M5.

The new age determination on the latest lava flows now dates all Stratum A deposits from 1.8 Ma to less than 1.78 Ma, the upper limit based on the paleomagnetic reversal from the latest Olduvai subchron to the early Upper Matuyama Chron clearly recorded in the M5 section (Ferring et al., 2011). This more precise shorter chronology for Stratum A is in better accord with the sedimentary-soil features of those deposits which, as discussed below, are indicative of rapid deposition separated by brief intervals of weathering and erosion.

3.2. Paleomagnetism

New results from M6 and M11 provide again a very stable demagnetization of samples as evidenced by orthogonal demagnetization plots (SOM Figs. S5−S8). The M6 section displays an entirely reverse polarity succession, whereas in M11, both normal and reverse polarities are identified for A and B strata, respectively (SOM Fig. S8).

These new data add to the records from Block 2 (Lordkipanidze et al., 2007) and M5 (Ferring et al., 2011) showing clearly that the Mashavera Basalt and Stratum A fall within a normal polarity chron correlated to the Olduvai subchron, and that Stratum B falls within a reverse polarity chron obviously correlated to the upper Matuyama Chron. The large number of polarities compiled in

stereoplots (SOM Fig. S8) provide an unprecedented and robust data set of strata A and B polarities. In addition, polarities reinforce the differentiation of A and B strata based on a geophysical parameter independent from sedimentological and textural descriptions and analyses.

3.3. Geoarchaeological contexts and formation processes

Above the Mashavera Basalt, sediments of the Dmanisi Formation have been divided into a stratified series of three formation contexts, defined based on geomorphic-sedimentary facies: 1) Stratum A, 2) Stratum B1, and 3) Strata B2–B5. Each of the three has eolian-colluvial slope facies, but over a large area of the upper promontory, Stratum B1 preserves a unique geologic record of a brief phase of piping and gullying that is not only unique in Paleolithic geoarchaeology but also was the context for accumulation and preservation of thousands of fossils including all of the bones of early *H. erectus* recovered at Dmanisi. After describing the Mashavera Basalt substrate surface, data for the three sedimentary units are presented that are used to characterize the facies of each unit, their sedimentary-geomorphic environments, and then weathering and soil development. Later discussion reviews the formation contexts for the three sedimentary units.

Mashavera Basalt The surface relief of the basalt was a controlling factor in the accumulation of the Dmanisi Formation deposits in two ways. At a larger scale, the basalt has a terrace-like configuration, with an upper promontory bench and a lower promontory bench that are separated by a steep (15–30%) slope (Fig. 1; Table 1). On the smaller scale, the upper promontory basalt surface has 2–3 m deep depressions that accommodated thicker accumulations of Stratum A deposits that were hosts for pipes and gullies. Excavations in Blocks 1 and 2, M5 and M17 have exposed slabs of basalt that were supported by A1 ashes and collapsed when that support was removed by erosion (SOM Fig. S9). This shows that the first A1 ashes were deposited before and very likely during the last lava flows on the promontory. A1 ashes under those collapsed slabs, as far as could be safely reached, were sterile. Continued Stratum A deposition filled the depressions and buried the basalt, as discussed next.

Stratum A Sediments of Stratum A not only preserve the oldest artifacts and faunas at Dmanisi (Ferring et al., 2011) but also served as the host sediments for pipes and gullies that filled with Stratum B1 deposits. Stratum A deposits have been exposed in all complete profiles with Dmanisi Formation strata except M6 (Figs. 1 and 2); the highest exposure is M19, where A1 and A2 overlie weathered Cretaceous bedrock (SOM Fig. S10), whereas at M15, the contact with the basalt is 13 m lower. The complete A1–A4 sequence is only exposed in M5, D1A, and M2, whereas Stratum A was truncated by erosion and/or Medieval disturbance in all other profiles (Figs. 2 and 3).

The boundary between A1 and A2 is gradual, but the A3/A2 and A4/A3 contacts are erosional and usually have rip-ups of the subjacent stratum just above the contact. Textures throughout Stratum A are quite uniform, with loamy sands in the basal deposits (A1–A2b) and sandy loams above (SOM Tables S2–S5). Although Fourier-transform infrared spectroscopy showed trace amounts of kaolinite throughout Stratum A (Ferring et al., 2011), pipette analysis showed these sediments to be almost clay-free, with <1% in just a few samples (Crislip, 2013); similar results were obtained by Garcia (2004). However, both crystalline and amorphous products of volcaniclastic weathering including allophane, imogolite, halloysite, and gibbsite need investigation at Dmanisi (Buurman et al., 1997; Chadwick et al., 2003; Jongmans et al., 1995; Zehetner et al., 2003). The absence of downslope fining of A sediments from M5 to Block 2 to M9 (Figs. 2 and 3; SOM Tables S3, S5 and S6) suggests that promontory-wide eolian sedimentation was more important than significant colluvial redeposition from the upper to lower promontory.

Mafic ashes dominate Stratum A sediments, ranging from 86 to 98% of identified clasts (Fig. 4; SOM Fig. S11; SOM Tables S7 and S8). Glass shards, commonly with plagioclase phenocrysts, predominate, with less common plagioclase and rare clinopyroxene crystals. EDS analysis of samples of plagioclase crystals from Strata A2, A3, and A4 yielded Ca/Na ratios of 0.81, 0.85, and 0.83, respectively (Crislip, 2013); this indicates high susceptibility to weathering. From 55% to almost 90% of the pyroclasts exhibit etching and/or pitting (Fig. 4), but that can occur relatively soon after deposition, especially in porous sediments (White and Brantley, 2003). Lithic clasts from Stratum A include very low frequencies of basalt, schist, quartzites, and FeMn oxides (SOM Table S8).

Soil morphology in all substrata is weakly developed. Color differences between substrata mainly reflect the mix of pyroclast colors (black, reddish brown, and clear) rather than pedogenic rubification (SOM Table S2). Substratum A1 is soft and friable and in M5 has a few thin lenticular beds. A1 grades into A2, which is very hard and has subangular blocky structure; A3 and A4 are firm and massive (SOM Table S2). Important with respect to piping, porosity is highest in the lower substrata and decreases continuously upward (Fig. 3a). No argillans occur in A sediments, and illuvial clay pore linings are only common in Strata A2a–A2b and rare above (SOM Table S7). Pedogenic carbonates occur mainly as pore linings, exhibited in profile as filaments, probably associated with fibrous roots of grasses (Messager et al., 2010; SOM Table S7). Carbonate rhizoliths, probably associated with shrub roots, are present in A2a and A4a. Overall, A2 has the best-developed soil morphology in Stratum A. Importantly, the weak soil morphology of Stratum A4 indicates a brief period of surface stability and weathering preceding the erosion at the A4/B1 contact.

The most common bioturbation features are krotovina (filled micromammal burrows), 3–4 cm in diameter, that occur in low frequencies in Strata A2b and A3, but are very common in Stratum A4, which also has areas with much larger micromammal galleries

Table 1
Slopes (%) on transects across the promontory.[a]

Stratum	M5–M16 section				M5–M15 section				
	M5–D1A	D1A–M8	M8–M9	M9–M16	M5–Blk 1	Blk1–Blk2	Blk2–M2	M2–M14	M14–M15
B3	3.83	5.77	7.39		1.65	10.71			
B2	4.00	6.73	7.27		3.66	6.12	7.35	5.73	
B1	3.50	7.69	8.41		3.30	4.59	8.46	6.81	
All A	2.67	1.92	10.45		2.56	2.04	8.82	10.93	38.85
A2	2.33	1.92	10.45		1.10	2.04	17.65	5.56	11.31
Basalt	8.50	−7.21	15.00	−6.12	0.37	2.04	30.88	1.43	11.15

[a] See Figure 1 for profile locations. Slopes were measured from top of strata. Negative slopes are rises.

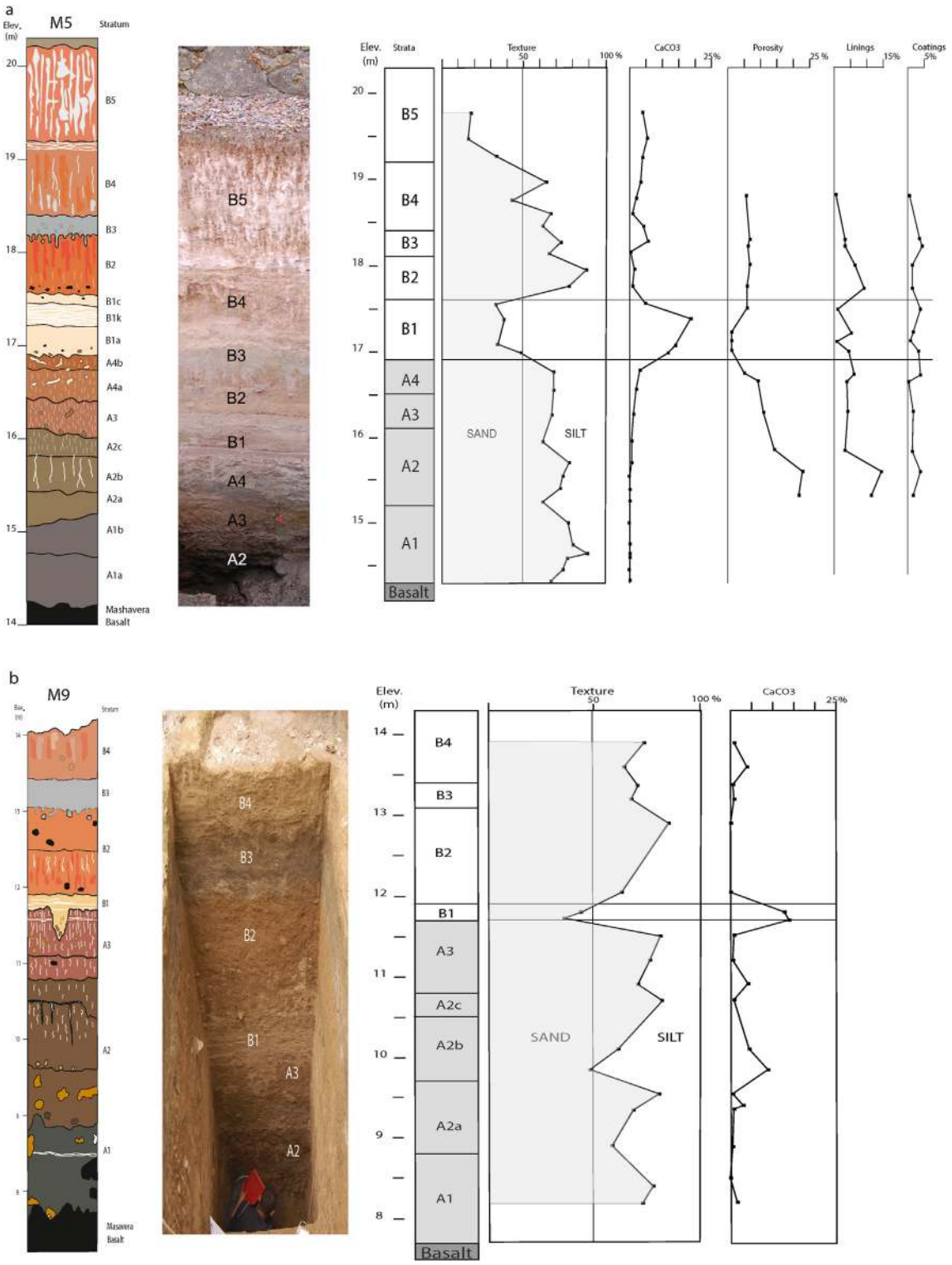

Figure 3. Stratigraphy and sedimentary-pedogenic data from the M5 and M9 sections. a) M5 is the type section for the Dmanisi Formation (Ferring et al., 2011). Both M5 and M9 exhibit only slope facies, whereas extensive pipe and gully facies of Stratum B1 are present over much of the upper promontory (Fig. 2). b) The M9 section has textural lithofacies very similar to those in M5, despite its location 210 m downslope from M5. Abbreviation: Elev. = elevation.

(SOM Table S2; SOM Fig. S12). The krotovina in A4 are filled with soft, calcareous B1 sediment, and have thin, hard carbonate linings. Fewer smaller (1 cm or less) vertical to subvertical burrows are probably from insects, such as the abundant burrowing wasps we see active all over the promontory today. Large mammal burrows into Stratum A and filled with B1 sediment will be discussed below.

By the end of Stratum A deposition, the depressions on the upper promontory basalt were all filled with Stratum A sediments, and the intervening areas with higher basalt had low

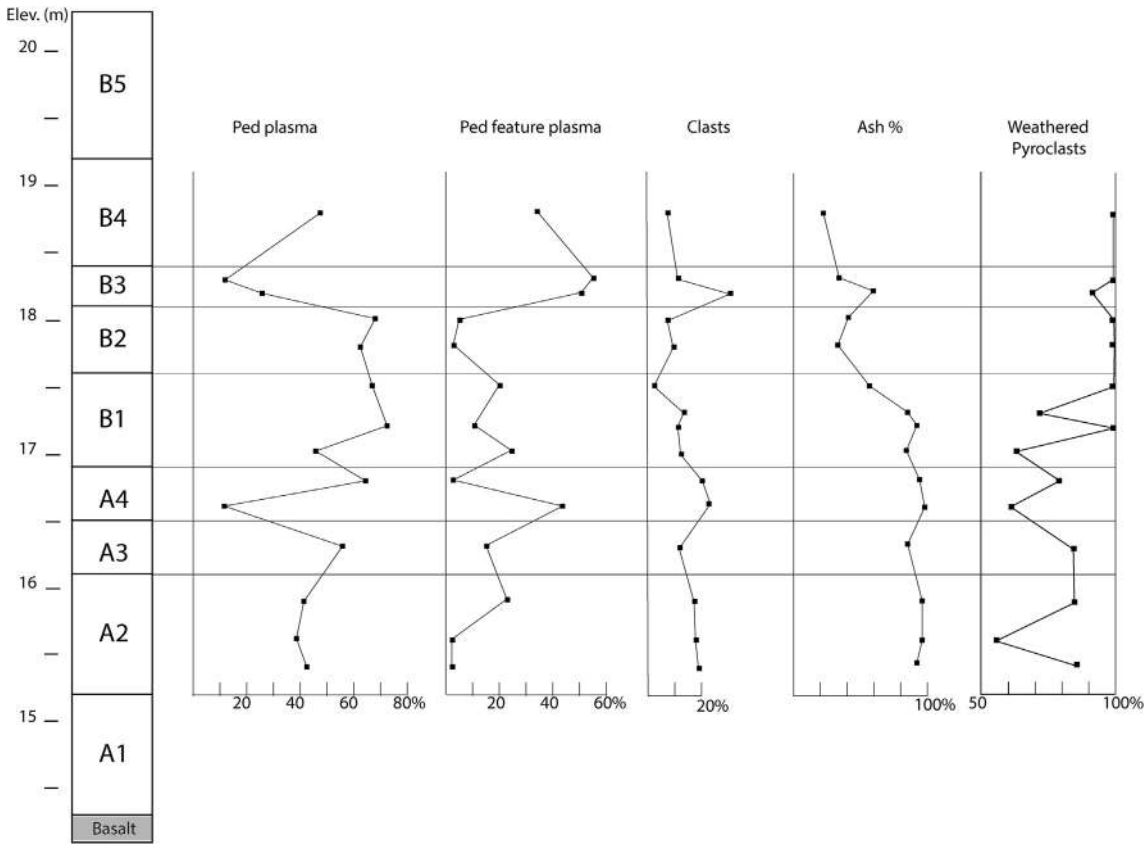

Figure 4. Composition and weathering data from point counts in the M5 section. These data derive from point counts of 15 thin sections made on samples from the M5 profile (SOM Tables S7 and S8). Additional soil features are shown in Figure 3a. These data show the dominance of plasma in all strata and overall trend of decreasing ash content among identified clasts and the increased proportion of weathered clasts in Stratum B compared to Stratum A. Abbreviation: Elev. = elevation.

slopes (2–2.5%) and Stratum A slope facies (Fig. 5b; Table 1). Slopes on the lower promontory are steeper, yet thick accumulation of Stratum A deposits in M2 and M9 shows the potential for preservation of superposed occupation surfaces over the large lower promontory area. Analyses are in progress on artifacts and faunas recovered from Stratum A deposits in Units M2, M14, and M9.

The Stratum A deposits filling the depressions on the basalt set the stage for the major changes in formation settings that were to follow. These deposits were ideal for pipe formation, having soft, massive loamy sands of A1 at the base, overlain by much harder, but very porous Stratum A2. The sandy loam to loamy sand textures of Stratum A sediments would have been conducive to infiltration and percolation (Fig. 3; Tejedor et al., 2012), further enhanced by the many macropores: rootlet pores, invertebrate burrows, and krotovina.

Erosion and piping commenced after deposition of A4. The weak soil features of A4 leave no evidence for a long period of surface stability and weathering. A4 has been thinned in several sections and removed in M9 (Figs. 2b and 3b). However, the widespread preservation of most Stratum A sediments suggests a brief erosional phase separates A4 from B1.

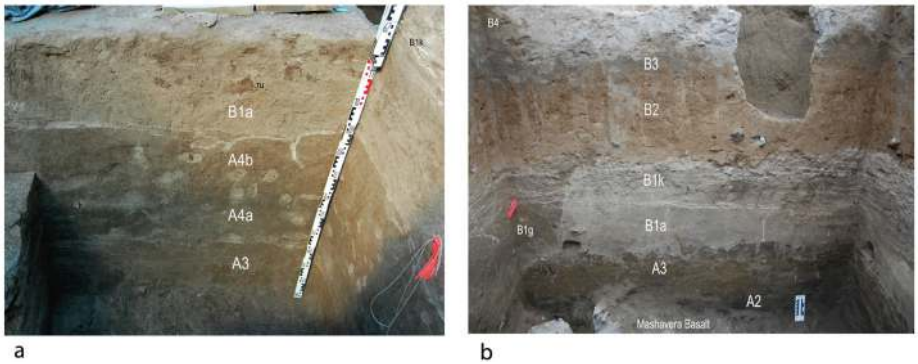

Figure 5. Photos of the Strata A/B unconformity. These profiles show the abrupt erosional contact of Stratum B1 slope facies with Stratum A. a) In this M5 profile, note the A4 rip-ups in B1a, the numerous krotovina (k) in A4 filled with B1 sediment, and the abrupt A4/A3 contact below; b) the bioturbated contact near the southwestern corner of Block 1 is above thinned and eroded A2 and A3. The slope facies of B1 here is typical for the high basalt surfaces on the upper promontory. Note the late rill/gully (B1g) inset against B1, similar to the B1x gully in Block 2 (Fig. 9a).

3.4. Stratum B1

Pipe initiation There are several lines of evidence bearing on the question of why piping was initiated at Dmanisi. First, the Stratum A substrate presented ideal contexts for piping. The silt-rich sediments, their weak soil morphology, high porosity toward their base, and the abundance of macropores resulting from biological activity are all factors that contribute to pipe initiation (Bernatek-Jakiel and Poesen, 2018). The large gully in M6 and the steep change in slopes at the edge of the upper promontory provided outlets for pipes to discharge their sediment. Last, the quite abrupt change in phytolith assemblages in the middle of Stratum A4 to compositions indicative of a shift to higher water stress and reduced tree cover (Messager et al., 2010) immediately precedes the erosion of Stratum A and appearance of pipes. The extremely sharp erosional contact between A4 and B1 at M5 not only suggests that surface was devegetated but also raises the possibility that it was deflated (Fig. 5a). Despite the apparent shift to drier environments at the A/B boundary based on botanical evidence, large faunal populations are indicated by accumulation of the abundant and diverse faunas in Stratum B1 (Bartolini-Lucenti et al., 2022), and there is no break in the hominin use of the promontory (Ferring et al., 2011).

Ultimately, the onset of piping had one immediate impact: the creation of new and unique contexts for site formation on the promontory, accompanied and followed by episodic deposition that resulted in preservation of an exceptional record of paleopiping in the middle of Dmanisi's stratigraphic sequence (Figs. 6 and 7).

These unique formation contexts at Dmanisi preserve the great majority of bones, including all of the hominin fossils recovered thus far (Coil et al., 2020; Gabunia et al., 2000; Lordkipanidze et al., 2007, 2013). The descriptions that follow show the marked variability in Stratum B1 geomorphic-sedimentary features that have been exposed by excavations on the upper promontory. Halliday's (2007) characterization of piping features as 'pseudokarst' is quite applicable here because Dmanisi's pipe features include subterranean tunnels that often connected to the surface via breaches, and also collapsed along their length, becoming gullies (Fig. 6).

Slope facies This facies covers areas of high basalt (Fig. 5b) and also overlies the thick Stratum A deposits in depressions (Figs. 3, 5a and 7). Slope facies of B1 have noticeably higher silt and carbonate content than Stratum A deposits (Fig. 2, SOM Tables S3, S5 and S6). Mean ash content decreases from 93.40% ($n = 6$) in A sediments to 78.91% in B1 ($n = 4$), with tuff, basalt, schist, and metaquartzite among the lithic clasts (SOM Table S8). The thickness of B1 slope facies at M5 as well as stratified artifacts in that stratum suggest that B1 ashes accumulated episodically, although both bioturbation and sedimentation on probable grassy surfaces obscured evidence of discrete depositional structures in field profiles as well as thin sections (Crislip, 2013; Ferring et al., 2011; Mallol, 2004; Zack, 2013). B1 slope facies are very thin in profiles M2 and M9 on the lower promontory (Table 1; Fig. 3a; SOM Figs. S13 and S14; SOM Table S9). The steeper slopes on the lower promontory probably increased erosion following B1 deposition.

Krotovina are very common within B1 slope facies. As mentioned earlier, these not only disturbed the A/B1 contact (Fig. 5b) but also penetrate into Stratum A (Fig. 5a). Construction and then filling of these burrows could easily have moved small bones and artifacts in both directions across the contact. Larger burrows associated with Stratum B1 are discussed below.

Pipe fill facies Filled pipes have been exposed in D1A–B (Figs. 7b and 8c; SOM Table S10), M8 (Figs. 7d and 8a), Room 11 (Fig. 8b), as well as M11 (not shown) and eastern Block 2 (SOM Fig. S15). The D2280 cranium was in a filled pipe in Block 1 (Gabunia et al., 2000; Jöris, 2008). Pipe fill sediments are readily distinguished from the

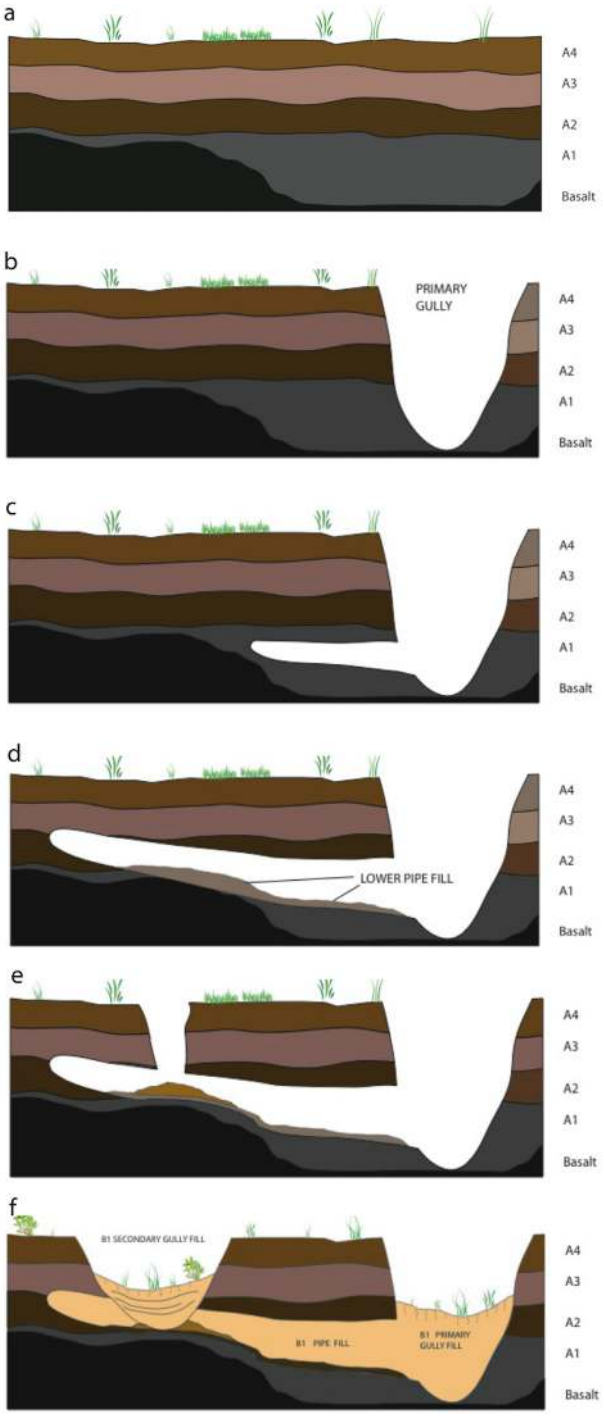

Figure 6. Model of pipe formation at Dmanisi. a) Stratum A ashes fill in depressions on the basalt surface, with soft A1 ashes facilitating pipe initiation. b) Primary gullies extend upslope by probable headcut retreat, creating gully wall outlets for pipe sediment. c) Pipes are initiated by infiltration and lateral flow of water. d) Pipes expand and lengthen by erosion and mass movement within the pipe, leaving lower pipe fill on pipe floor. e) Breaching (collapse) occurs as pipe roof thins, enabling direct overland flow into the pipe, accelerating pipe growth and enabling deposition of bones and stones from surrounding surface into the pipe. f) Continued pipe collapse created blind valleys, or open gullies that flowed downslope to the east. Note all pipe and gully features filled with B1 sediment. See Figure 7 for pipe and gully features north of Blocks 1 and 2.

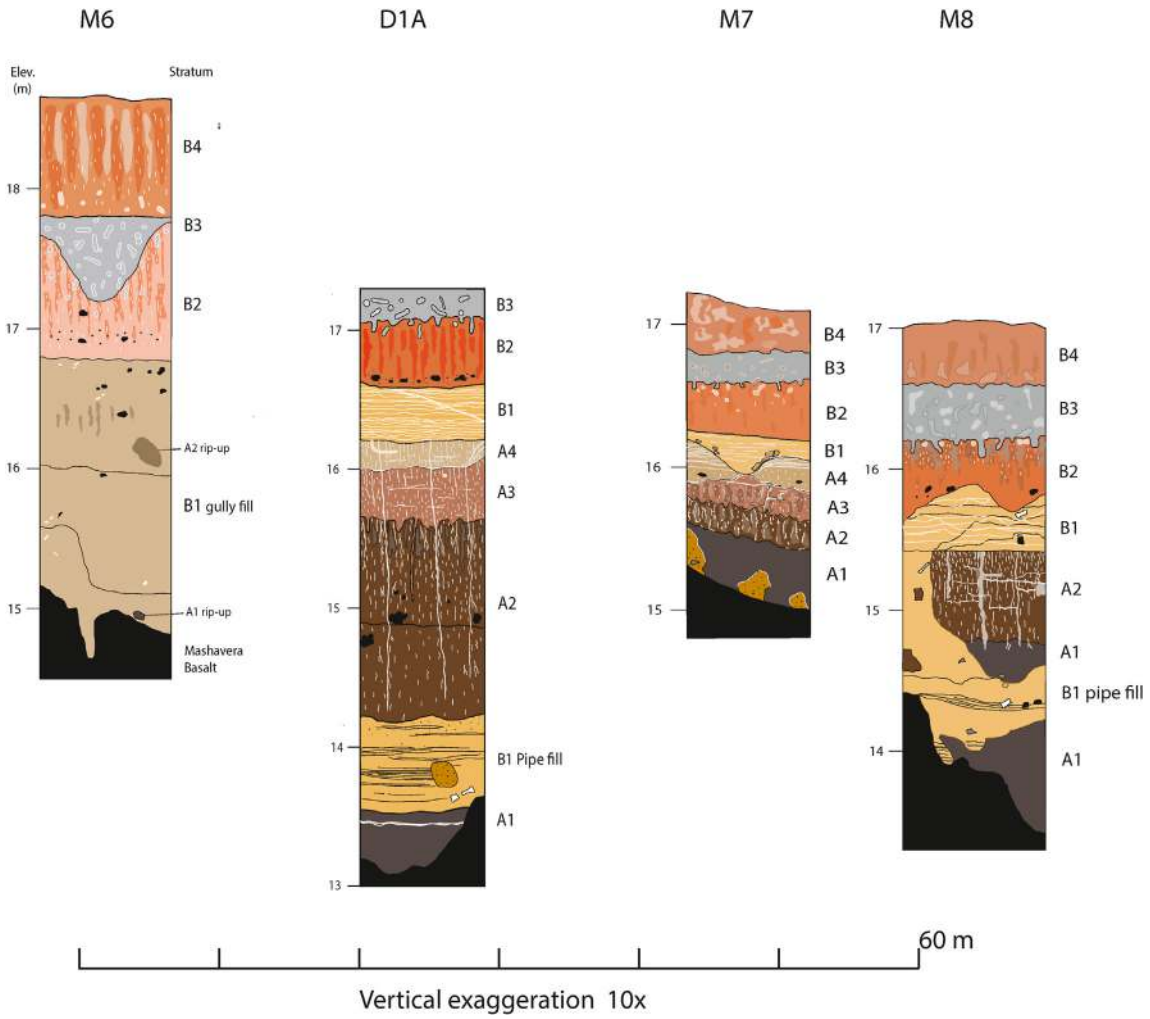

Figure 7. Section of profiles north of Blocks 1 and 2 showing gully and pipe features. These profiles illustrate the contexts and results of gullying and piping on the upper promontory (see Fig. 1c for locations). The M6 primary gully provided a gully wall exit for sediments removed from the pipe in D1A. The fully exposed pipe adjacent to D1A was filled with B1 sediment, with numerous bones in the lower pipe fill. Note that B1 slope facies surmount Stratum A deposits here. High basalt in M7 resulted in thinner Stratum A deposits and sheetwash toward the lower promontory. The pipe in M8 was breached and then filled with B1 sediment with bones, stones, and rip-ups of Stratum A2 in the pipe fill. Note the erosion of B1 in the M8 profile, and the uniform burial of B1 deposits by B2–B4 in these four profiles. Abbreviation: Elev. = elevation.

Stratum A host deposits based on color, the presence of laminations or thin beds, as well as angular to subangular rip-ups of both Stratum A host deposits and Stratum B1 slope facies. Lower pipe fills contain higher proportions of reworked stratum A1 ashes. Pipe fills also contain bones and usually cobbles that washed in from B1 surfaces surrounding breaches (Fig. 8b, c).

Pipe breach facies Several of the exposed pipes were breached, caused by collapse of a portion of the pipe roof. The breach in M8 was at least 1.4 m in diameter (Figs. 7d and 8a). The breach partially exposed in the southeast corner of Block 1 (SOM Fig. S16) is constricted where it passed through hard Stratum A, similar to one in southern Block 2 (not shown). In all cases, the fill of the breaches is B1 sediment. All of the breaches and the surrounding Stratum A host deposits are capped by B1 slope facies, indicating that breaching preceded and/or accompanied B1 deposition.

Collapse gully facies The elongated segments of collapsed pipes are called collapse gullies here, but are the same as the blind gullies of Bernatek-Jakiel and Poesen (2018). These occur in eastern Block 1 (Fig. 8d), northern Block 2 (Fig. 9), and M11 (SOM Fig. S17). Having formed in collapsed pipes, it is not possible to reliably discern lower gully fill from remnant lower pipe fill as in the filled pipe in Profile D1B (Fig. 8c). In all cases so far, thin deposits of the distinctive black ashes of A1 separate the gully fills from the basalt (Fig. 8d). The gully fills include thin, lenticular beds with massive to laminated gravelly sandy loam to loamy sand containing many rip-ups of B1 and Stratum A sediments (SOM Table S6). In Block 2, the gully deposits contain thousands of animal bones, including many small fragments. Bone taphonomy and elongated bone orientations indicate very low flow velocities; nearly vertical orientations of some long bones suggest they were entrained in saturated mudflows (Coil et al., 2020). The only soil features of these deposits are carbonate filaments, while truncated rhizoliths show that thin beds must have been separated in time by at least one growing season.

Large gully facies Large gullies constitute a potentially extensive formation context at Dmanisi. Two large gullies flank the main excavation areas, flowing downslope to the lower promontory. The first is at the southern end of the Room 11 profile; this has been covered by backfill since the early 1990s, and is shown somewhat schematically in Djaparidze et al. (1989). That gully provided an outlet for the nearly continuous series of filled pipes at the base of the Room 11 profile (Fig. 8b). Only the fill of the second gully has been exposed in M6, where thick B1 ashes extend to the basalt

Figure 8. Photos of Stratum B1 pipe facies. These profiles are examples of variations in pipe facies, including the strong contrast of their fill with the surrounding Stratum A host deposits. a) The profile in M8 has a breach filled with B1 sediment containing bones and many rip-ups of A2 extending down to the filled pipe (see Fig. 7). B1 was eroded after formation of the laminated calcrete before deposition of B2. Note the tensional cracks with micritic fill in A2. The steeply dipping basalt accommodated thick A1 and A2. b) This is one of several filled pipes near the base of the Room 11 section that originate in southeastern Block 1 (see SOM Fig. S16). The filled pipes in Room 11 contained hundreds of bones and cobbles (Djaparidze et al., 1989) washed into the pipes from the B1 surface. c) This filled pipe exposed in cellar profile D1B undercut a large area of Stratum A and extends into the adjacent cellar D1A (Fig. 7). The pipe must have emptied into the deep gully that was exposed in M6 (Fig. 7; SOM Fig. S18). The lower pipe fill is B1 interstratified with reworked A1, and the upper fill contains large rip-ups of A2 and A3. Numerous bones in the lower fill suggest this large pipe may have been a carnivore den. d) This collapsed gully fill is in northeastern Block 1, 5 m from the western edge of the Block 2 profile shown in Figure 9a. The two profiles are separated by high basalt. Note the bedded and heterogeneous gully fill overlying a thin, distinctive remnant of A1 ashes. The pipe fill on the lower right extended into the breached pipe that contained the D211 mandible and D2280 cranium (Gabunia and Vekua, 1995; Gabunia et al., 2000). Krotovina and many carbonate veins extend into the fill from the upper fill with the laminated calcrete (B1k). See Figure 1 for locations.

surface (Fig. 7a; SOM Fig. S18; SOM Table S11). It is assumed that the M6 gully provided an outlet for the D1A-filled pipe (Fig. 7b).

In addition to artifacts, the B1 fill of the M6 gully has extremely high densities of bones as well as rounded cobbles and rough clasts eroded from the Mashavera Basalt (Shelia et al., 2020; SOM Fig. S18; SOM Table S11). Three hominin fossils from the gully fill include the tooth from which proteins were extracted by Welker et al. (2020). As in M6, the collapse gully in Block 2 had artifacts, thousands of bones as well as many cobbles (Coil et al., 2020). In M18, just north of M6, similar thick B1 ashes contained a few cobbles, and many bones, which became so dense that excavations were stopped pending expansion to a block (SOM Fig. S19; SOM Table S12). Profile M14 on the lower promontory has thick B1 deposits with quite high densities of artifacts and cobbles, suggesting that it may be in or at the edge of a large gully that presumably drained from the upper promontory (SOM Fig. S20; SOM Table S13).

Stratum B1 cobbles The cobbles in B1 deposits (as well as Stratum B2, discussed later) present a geologic enigma. Cobbles are found in B1 ash matrix in both gully and slope facies over the upper and lower promontories. The lithology of those cobbles shows that most derive from the Pinesauri drainage, which is the only source for the plutonic and metamorphic lithologies for both the B1 cobbles and the modern Pinesauri gravels (SOM Figs. S1 and S21; SOM Table S14). No colluvial source for those cobbles, such as terrace gravels, has been found above the promontory. The high densities of larger cobbles (>5 cm in length) are accompanied by much greater numbers of clasts 0.3–5 cm in size (SOM Fig. S22; SOM Table S15). An obvious question is how could so many quite large cobbles be deposited in gullies along with thousands of bones that show no evidence of fluvial transport, as shown by data from Block 2 (Coil et al., 2020) and M6 (Shelia et al., 2020). Because the larger cobbles include raw materials used for artifact manufacture (Ferring et al., 2011; Mgeladze et al., 2011), the analysis of these materials requires comprehensive analysis of raw material selection that is beyond the scope of this article.

Stratum B1 large burrows In addition to krotovina, evidence of burrowing by larger animals is evident in several excavation areas. Burrows 15–30 cm in diameter were exposed in the collapse gully

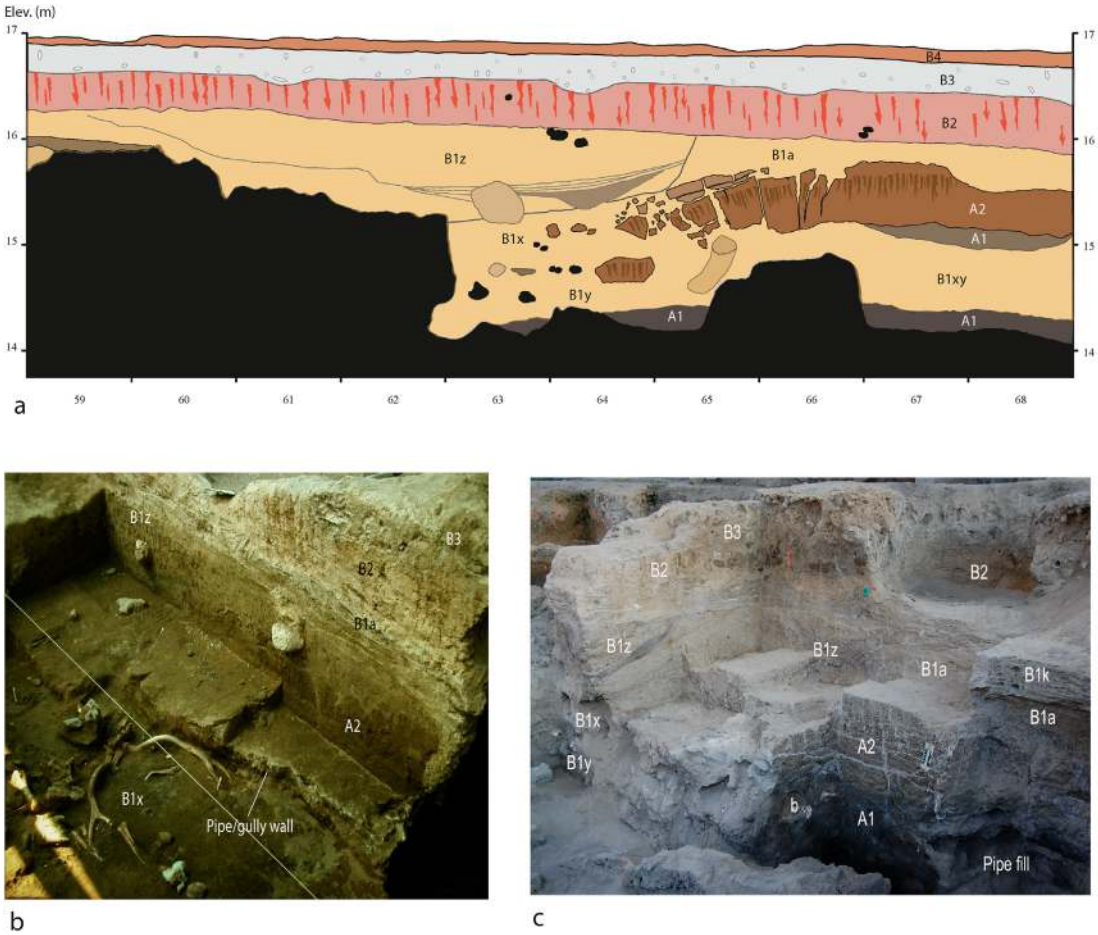

Figure 9. Cross-section and photos of northern Block 2 during excavation. a) The pipe that formed in the basalt depression flowed to the east (right) and became a gully following collapse of the A1/A2 pipe roof. The B1a slope facies aggraded before pipe collapse and the pipe and gully fills have rip-ups of B1. Rip-ups of A1 and A2 in B1x and B1y may have come from the pipe walls or the later gully walls. Note the medium and large mammal burrows (light brown) in the B1x-z deposits. b) The B1x gully deposits are inset against the former pipe wall; B1x and the B1y below contained several thousand animal fossils and about 65 hominin bones recovered in Block 2 (see text for discussion). The Cervid skull with attached antlers is one of two found at this level of the gully floor as it filled, surrounded by other fossils, artifacts, and numerous rounded cobbles; c) the perpendicular profile intersects the cross-section in Figure 9a. Note the steeply dipping thin beds of B1z that merge with B1x, and the preserved pipe fill below A2 and A1. Abbreviation: Elev. = elevation.

fill in Block 2 (Fig. 9a), and more recent excavations have exposed a much larger (>70 cm diameter) burrow cut longitudinally by the east wall of Block 2 (SOM Fig. S15). The B1 fill of this burrow was truncated by erosion, showing that Stratum B1 must have been thick enough to host such a large burrow before the erosion. Similar-sized burrows have been found in Block 3 (SOM Fig. S23), and the marked disturbance in southeast Block 1 was probably the result of large animal burrowing as well (SOM Fig. S16). Three large burrows containing many gnawed bones extended into Stratum A deposits in M5. All these large burrows into Stratum A not only disturbed those deposits but also must have brought Stratum A sediments to the B1 surface where they probably contributed to the frequent reworked Stratum A aggregates found in virtually all facies of Stratum B1.

Laminated calcrete Laminated calcrete formed in the upper part of all facies of Stratum B1 (SOM Fig. S24). The older stratigraphic scheme did not recognize these as postdepositional features and called this horizon 'Stratum III' (Djaparidze et al., 1989; but see Jöris, 2008). These are thin, anastomosing micritic laminae that have some pseudomorphs of plant tissues (Mallol, 2004). These calcretes cross all contacts between B1 facies (see Figs. 5b and 9a) including the large burrow in Block 2 (SOM Fig. S15). The calcretes functioned as a hardpan and an aquitard that largely if not completely prohibited meteoric waters' percolation to deeper deposits. There are no cases in which the calcretes have been cut through by younger deposits, virtually precluding introduction of fossils or artifacts from higher strata into B1.

The B1–B2 boundary Erosion between Strata B1 and B2 clearly reached the top of the laminated calcrete on the upper promontory (Figs. 5b, 7d and 8a; SOM Fig. S15), but not at M5 (Fig. 3a). As mentioned earlier, the truncated larger burrow in Block 2 (SOM Fig. S15) indicates modest erosional loss of B1, but no real estimate can be made. Nonetheless, that erosion would easily have removed artifacts and faunas from B1 above the laminated calcrete. After the erosion, deposition of slope facies begins with B2 and continues for the rest of Dmanisi's stratigraphic sequence.

3.5. Strata B2–B5

Following deposition of the complex facies of Stratum B1, Strata B2–B5 aggrade on the upper and lower promontories entirely as slope facies, with no evidence of pipes, gullies, or large burrows. Slopes of strata B1–B3 show no major adjustments from M5–M8–M9, but the slopes from Block 1 to Block 2 increase,

presumably resulting from erosional thinning near the edge of the upper promontory (Table 1). Although Strata B4 and B5 are poorly preserved or absent in many profiles, the widespread burial of B1 by B2 and B3 show clearly that no intrusive disturbances have affected the many bones, artifacts, and hominin fossils in B1 (Figs. 2 and 7). Moreover, the slope facies of B2–B5 preserve stratified artifacts and faunas, extending the stratigraphic range for the study of paleoenvironments as well as variability and change in occupation patterns at Dmanisi (Ferring et al., 2011).

Strata B2–B5 differ from all of those below in terms of sediment lithology as well as weathering and soil morphology. The silts in Stratum B5 cap a fining upward pattern for the <2 mm fraction at M5, whereas the textures of B2–B4 in M9 are comparatively consistent, and very similar to those of Stratum A (Fig. 3). However, the lithology of B2–B4 sediments in M5 is quite different from Stratum A (Fig. 4; SOM Tables S7 and S8), with lower ash content and higher frequencies of tuff, basalt, schist, and quartzite clasts. This points to an increased Pinesauri drainage source for these fine-grained clasts, similar to that of the high density of cobbles, pebbles, and granules in lower Stratum B2 (SOM Figs. S22 and S23; SOM Tables S14 and S15). All of the slopes above the promontory are Cretaceous bedrock, and no terrace deposits above the site have been found. Nonetheless, the cobbles and smaller gravels in lower B2 form a matrix-supported gravel sheet over the whole promontory. Bioturbation probably contributed to the concentration of larger cobbles (and artifacts) in lower B2, creating a biomantle (Johnson, 1989, 1990).

Soil morphology in Strata B2–B5 is quite different than for the strata below, including differences in color, structure, pedogenic carbonates, and argillans (Fig. 3; SOM Table S2). Except for B3, these strata all exhibit moderate to strong structure, with well-developed prismatic structure in B5. Pedogenic carbonates increase upward, including a laminated petrocalcic horizon at the top of B4 and very prominent vertical carbonate masses in B5 (Fig. 3; SOM Table S2). There are many argillans in B2, and both argillans and mangans in B5. Strata B2–B3 have quite high porosity, with many pore linings of FeMn oxides in B2 (SOM Table S7). Significant bioturbation in Stratum B2 has left vertical remnants of an argillic or cambic horizon that we informally call 'pedorelics.' The distinctive gray color of Stratum B3 is the result of fresh, dark ashes. As in Stratum B1, these ashes have many prominent krotovina within the stratum and also penetrate down into B2 (Figs. 3, 7). Together, the light brown B2 and dark gray B3 are easily correlated across the promontory, and are good targets for spatial analysis of artifacts and faunas (Fig. 2).

4. Discussion

As a very large, deeply stratified site, the Dmanisi promontory presents the opportunity to recover and study records of serial occupations by early *H. erectus*. As well known by now, those records include many hominin fossils in direct association with thousands of artifacts and faunal remains. Although Dmanisi is already famous for its large number of well-preserved hominin fossils, this is a rare if not unique site, in terms of its potential to yield insights into the first adaptations to temperate environments as part of the early colonization of Eurasia. That potential, and the contributions that ongoing investigations may make, will be strengthened by careful study of the spatial and stratigraphic variability in geologic contexts and formation processes that condition the accumulation, burial, and preservation of archaeological and paleontological materials. Formation studies in northern Block 2 (Coil et al., 2020) and M6 (Shelia et al., 2020) illustrate examples of the complex facies of Stratum B1, in the middle of Dmanisi's full stratigraphy (Ferring et al., 2011).

The following discussion will focus on the formation processes for Dmanisi's entire stratigraphic record, organized around the stratigraphic units defined in the introduction: Stratum A, Stratum B1, and Strata B2–B5. For each of these units, the site formation processes discussed include those related to site construction and site modification (Butzer, 1982; Ferring, 1992). Site construction entails the accumulation and burial of artifacts and faunal remains. Site modification includes the effects of physical and chemical agents that alter those objects as well as their spatial–stratigraphic locations and associations (Lyman, 1994; Schiffer, 1983; Wood and Johnson, 1978).

4.1. Stratum A

The accumulation of Stratum A, including its four substrata A1–A4, is widely recorded on both the upper and lower promontories (Figs. 1 and 2). Textural, petrologic, and geomorphic data indicate that Stratum A sediments were all deposited by low-energy eolian processes, probably on well-vegetated surfaces. These were ideal conditions for the accumulation of intact, superposed assemblages of artifacts and faunas. Rates of sedimentation can only be estimated in a relative way, based on soil morphology. Stratum A2 has pedogenic structure indicative of early formation of a cambic B horizon, whereas the other substrata only exhibit pedogenic carbonates. This weak soil development among the substrata suggests rapid, episodic deposition, ideal for recovery of in situ artifacts and fauna.

The potential for stratified occupation horizons within substrata is largely determined by their thickness, which varies markedly depending on the basalt relief. Clearly stratified artifacts in A2–A4 were documented in testing at M5 (Ferring et al., 2011). Elsewhere on the upper promontory, thicker Stratum A deposits are preserved only in basalt depressions which probably received A sediment from surrounding areas with higher basalt, such as M7 (Fig. 7). Thus, the A sediments in those depressions may include bones and artifacts in secondary positions. The lower promontory appears to be a better place to recover in situ artifacts and faunas in Stratum A, based on their recovery from thick Stratum A deposits in test units M2 and M9.

The principal agents of disturbance in Stratum A are bioturbation and erosion. The few krotovina in Strata A1–A3 are indicative of a low degree of bioturbation by agents that could move bones and artifacts (Ferring, 1986). Burrowing by micromammals and also invertebrates could have enhanced rates of burial, but also created secondary concentrations of larger objects in the lower parts of biomantles (Johnson, 1989, 1990). Much more disturbance via bioturbation is evident in A4, as mentioned earlier. This may well have translocated smaller artifacts and bones in both directions from the A4/B1 contact (Fig. 5). Loss and/or mixture of materials by erosion is suggested by the clear to abrupt boundaries between A2/A3 and A3/A4, but thus far lag concentrations of artifacts have only been exposed at the A3/A4 contact in unit M2 (SOM Fig. S14; SOM Table S9).

4.2. Stratum B1

The diverse slope, pipe, gully, and burrowing facies of Stratum B1 each constitute distinct formation contexts. As shown in and near Blocks 1 and 2, the pipe and gully contexts were defined by the basalt relief. On the upper promontory, those contexts are discrete, small microbasins that have abrupt boundaries. For most archaeological sites, the pipe and gully-related contexts would be considered settings for destructive site modification processes. But at Dmanisi, they preserve thousands of bones and may actually have promoted bone accumulation by providing denning locations

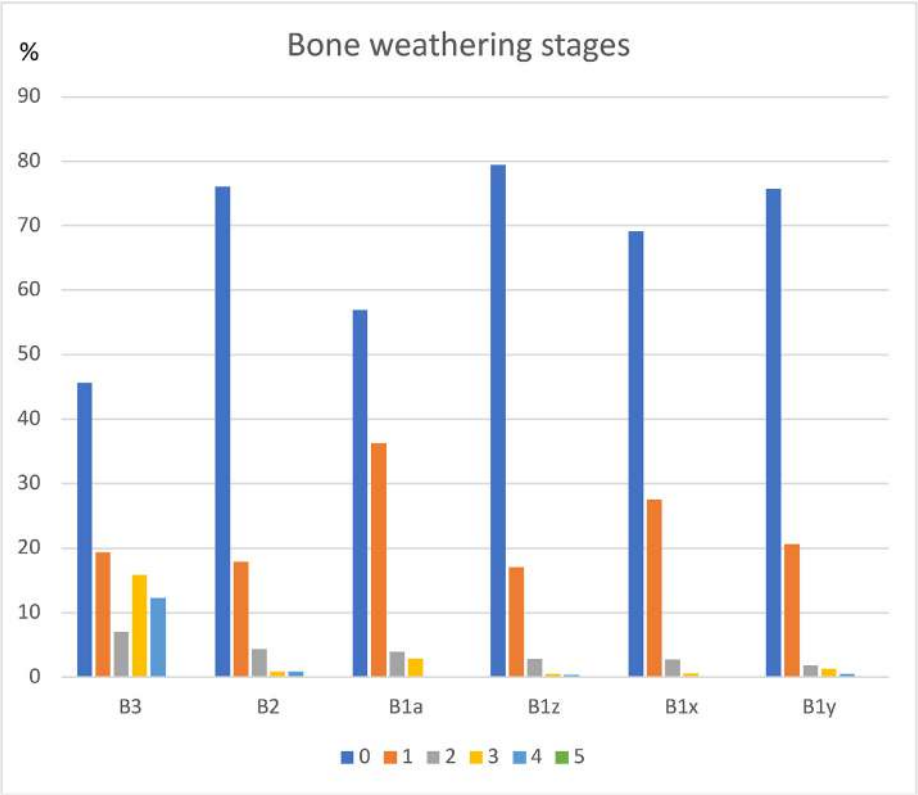

Figure 10. Weathering stages for bones in B strata from Block 2. These data show clearly the high proportions of bones in weathering stages 0 or 1 for all strata, indicating very short periods of preburial exposure (Behrensmeyer et al., 1978; SOM Table S16). For Stratum B1, these data support the short period estimated for rapid creation and filling of pipe and gully features on the upper promontory at Dmanisi.

for carnivores. Reconstructing whether the bones and artifacts were deposited in the open features (gullies and collapse gullies) or washed from surrounding B1 surfaces will be difficult. But they do represent assemblages in excellent stratigraphic context that were sealed from any possible later intrusive disturbances by Stratum B2.

Importantly, the B1 pipe and gully features probably formed and were filled in a matter of decades, based on documented life spans of pipes in many settings (Bernatek-Jakiel and Poesen, 2018). This time factor is supported by bone weathering stages of Stratum B1 deposits in Block 2 (Fig. 10; SOM Table S16). The high proportion of bones in Stages 0 or 1 indicates that even if a substantial number of the bones washed in from B1 surfaces, they had not been exposed for many years before being transported to the collapse gully in Block 2 (Behrensmeyer et al., 1978; Coil et al., 2020). Another indicator of the good bone preservation in Stratum B1 is the recovery of proteins from a rhinoceros tooth (Cappellini et al., 2019) and a hominin tooth (Welker et al., 2020). Overall, the pipe-related facies may be excellent settings to recover large samples of bones and certainly some in situ evidence for carcass processing could be preserved in the open features such as the collapse gully in Block 2 and the large gully in M6 (Coil et al., 2020; Shelia et al., 2020). Otherwise, these facies provided matrix for redeposited artifacts and faunas.

The large samples of faunas and the many hominin fossils recovered from pipe and gully facies have been the source of important research contributions at Dmanisi. But it is the slope facies of Stratum B1 that have the highest potential to preserve living surfaces with primary accumulations of artifacts and bones. This has been realized in M5, where superposed artifacts and sparse faunas have been recovered from B1 (Ferring et al., in prep). These opportunities should be quite widespread on the upper promontory, where quite thick B1 slope facies are present in almost all exposed profiles (Figs. 2, 5 and 7). Erosional loss of upper B1 appears to have increased toward the eastern edge of the upper promontory, but even there 40–50 cm of B1 slope facies are preserved. Syndepositional and postdepositional burrowing by micromammals have probably translocated smaller bones and artifacts, and at least one large burrow has been exposed in B1 in Block 2 (SOM Fig. S15). Nonetheless, the B1 slope facies are amenable to excavations over large areas ideal for spatial analyses. Unfortunately, the laminated calcretes make excavation and bone recovery very difficult, and heavy carbonate coatings on bone surfaces are common. As for some of the thicker A substrata, the B1 slope facies are the best contexts available for recovery of in situ occupation records. Fortunately, similar contexts can be defined for Strata B2 through B5.

4.3. Strata B2–B5

Strata B2–B5 are all slope facies. After B1, there is no evidence for pipes, gullies, or large animal burrows. The density of gravels in B2 certainly creates the impression of high surface flow velocities, but as stressed above, the mechanism of deposition has not been defined. Stratum B2 has the highest densities of lithic artifacts, which are in direct association with the gravels, but they show little evidence of edge damage. Many of the cobbles in B2 are the right size and raw material to be used as cores for manufacturing flakes (SOM Tables S14 and S15; Ferring et al., 2011; Mgeladze et al., 2011). A most unusual site formation process, this means raw materials were deposited on the site rather late in its occupation history, eliminating the need for longer distance stone transport by

hominins. Less intensive core reduction appears to have been a response (Ferring et al., 2011).

Aside from the gravel issue, Stratum B2 slope facies appear to have been conducive to the preservation of superposed artifacts and faunas on the upper promontory, and at least in M9 on the lower promontory. Although Stratum B2 soil morphology is stronger than in Stratum A or B1, bone weathering is virtually the same as in the B1 collapse gully facies (Fig. 10; SOM Table S16).

Stratum B3 is the highest that has been exposed over a large area (Figs. 1 and 2). The fresh dark ashes are distinctive but are usually thin, heavily bioturbated, and somewhat less weathered than the strata above and below. However, the small sample of B3 bones from Block 2 shows a slightly lower percentage of stages 0 and 1 than in B1 and B2 (Fig. 10). The strongly bioturbated boundary with B2 is difficult to follow during excavation, and B3 is usually too thin to expect stratified occupation surfaces within the stratum. Nonetheless, B3 provides another context for spatial study of occupations across much of the promontory.

The record of Strata B4 and B5 is poor, owing to loss by erosion and Medieval constructions, but their thickness in M5 suggests many serial accumulations of increasingly finer sediment (Fig. 3a). The fining upward textural trend is paralleled by evidence for increasing tree cover and reduced water stress (Messager et al., 2010), even though both strata have substantial pedogenic carbonate accumulations. Artifact and bone densities are very low in these strata, possibly reflecting decreased occupations in the M5 area, or increased sedimentation rates, or both. In any event, future investigation of these deposits will have to focus on the high upper promontory peripheral to M5.

5. Conclusions

Given its thick stratified deposits containing associated artifacts, faunas, and hominin fossils, the Dmanisi promontory would rank as a premier site at any time or place in the Lower Paleolithic record. Dmanisi was a strategic place on the early Pleistocene landscape of the Caucasus. It strides the confluence of two rivers that provide riparian corridors to volcanic highlands to the west and south and to the steppes of the Caspian Basin to the east: certain pathways for both large animals as well as humans. This setting was a crucial factor that attracted carnivores, herbivores, and humans to the promontory over some thousands of years between 1.80 and 1.76 Ma. Therein lies the first component of site construction: the accumulation of artifacts and associated faunal remains on a distinct landform.

This article documents the second component of site construction at Dmanisi: a series of stratified sedimentary contexts for the burial and preservation of artifacts and faunas over an area of at least 40,000 m^2 on the promontory. Geoarchaeological investigations reported here have defined two formation domains at Dmanisi that provide different yet integrated opportunities for research. Slope facies dominate that record over the whole promontory for all of Stratum A, an extensive part of Stratum B1, and all of Strata B2–B5. Although affected by bioturbation and episodic erosion, these facies provide excellent contexts for investigating spatial-stratigraphic variability among the many serial occupations of the Dmanisi promontory. These facies surround the second domain: the pipe and gully facies of Stratum B1 on the upper promontory that formed in microbasins on the basalt surface. Although the microbasins are quite poor places to expect intact living surfaces, they have proven to be invaluable contexts for the accumulation and preservation of large faunal assemblages as well as hominin fossils that are in secure stratigraphic context. Moreover, they also preserve evidence of carnivore denning and bone modification by both carnivores and hominins: key evidence of their interactions. The coordinated study of both of these domains highlights why research at Dmanisi continues to shed light on the first adaptations to temperate regions by early *H. erectus*.

Declaration of competing interest

None of the authors declare any competing interests.

Acknowledgments

We thank all of the Dmanisi team members from the Georgian National Museum as well as staff at the Dmanisi field camp for their efforts and hospitality. We thank Jordi Agustí and Lorenzo Rook for organizing this effort and including our contribution to the Dmanisi Project. This research was supported by NSF grants (numbers BCS-1025245, BCS-1019408). Fieldwork at Dmanisi was also supported by grants from the Leakey Foundation and the John Templeton Foundation. The technical support provided by the Paleomagnetism laboratory at GEO3BCN (SCTUB_CSIC, Barcelona) is much appreciated. O.O. belongs to research group 2017 SGR 1666.

References

Baena, J., Lordikpanidze, D., Cuartero, F., Ferring, R., Zhvania, D., Martín, D., Shelia, T., Bidzinashvili, G., Roca, M., Rubio, D., 2010. Technical and technological complexity in the beginning: The study of Dmanisi lithic assemblage. Quat. Int. 223–224, 45–54.

Bartolini-Lucenti, S., Cirilli, O., Pandolfi, L., Bernor, R.L., Bukhsianidze, M., Carotenuto, F., Lordkipanidze, D., Tsikaridze, N., Rook, L., 2022. Zoogeographic significance of Dmanisi large mammal assemblage. J. Hum. Evol. 163, 1–18.

Behrensmeyer, A.K., 1978. Taphonomic and ecologic information from bone weathering. Paleobiology 4, 150–162.

Bernatek-Jakiel, A., Poesen, J., 2018. Subsurface erosion by soil piping: Significance and research needs. Earth Sci. Rev. 185, 1107–1128.

Bernatek-Jakiel, A., Jakiel, M., Krzemień, K., 2017. Piping dynamics in mid-altitude mountains under a temperate climate: Bieszczady Mts., Eastern Carpathians. Earth Surf. Process. Landf. 42, 1419–1433.

Bryan, R., Jones, J., 1997. The significance of soil piping processes: Inventory and prospect. Geomorphology 20, 209–218.

Butzer, K.W., 1982. Archaeology as Human Ecology. Cambridge University Press, Cambridge.

Buurman, P., de Boer, K., Pape, T., 1997. Laser grain-size characteristics of Andisols in perhumid Costa Rica: The aggregate size of allophane. Geoderma 78, 71–91.

Cappellini, E., Welker, F., Pandolfi, L., Ramos-Madrigal, J., Samodova, D., Rüther, P.L., Fotakis, A.K., Lyon, D., Moreno-Mayar, J.V., Bukhsianidze, M., Rakownikow Jersie-Christensen, R., Mackie, M., Ginolhac, A., Ferring, R., Tappen, M., Palkopoulou, E., Dickinson, M.R., Stafford Jr., T.W., Chan, Y.L., Götherström, A., Nathan, S., Heintzman, P.D., Kapp, J.D., Kirillova, I., Moodley, Y., Agusti, J., Kahlke, R.-D., Kiladze, G., Martínez-Navarro, B., Liu, S., Sandoval Velasco, M., Sinding, M.-H., Kelstrup, C.D., Allentoft, M.E., Orlando, L., Penkman, K., Shapiro, B., Rook, L., Dalén, L., Gilbert, T.P., Olsen, J.V., Lordkipanidze, D., Willerslev, E., 2019. Early Pleistocene enamel proteome from Dmanisi resolves *Stephanorhinus* phylogeny. Nature 574, 103–107.

Chadwick, O.A., Gavenada, R.T., Kelly, E.C., Ziegler, K., Olson, C.G., Elliot, W.C., Hendricks, D.M., 2003. The impact of climate on the biogeochemical functioning of volcanic soils. Chem. Geol. 202, 195–223.

Coil, R., Tappen, M., Ferring, R., Bukhsianidze, M., Nioradze, M., Lordkipanidze, D., 2020. Spatial patterning of the archaeological and paleontological assemblage at Dmanisi, Georgia: An analysis of site formation and carnivore-hominin interaction in Block 2. J. Hum. Evol. 143, 1–16.

Crislip, P.S., 2013. A quantitative assessment of site formation at the Dmanisi Archaeological Site, Republic of Georgia. M.Sc. Thesis, University of North Texas.

de Lumley, M.-A., Lordkipanidze, D., 2006. L'homme de Dmanissi (*Homo georgicus*) il y a 1 810 000 ans. C. R. Palevol. 5, 273–281.

Djaparidze, D., Bosinski, G., Bugianishvili, T., Gabunia, L., Justus, A., Klopotovskaja, N., Kvavadze, E., Lordkipanidze, D., Majsuradze, G., Mgeladze, N., Nioradze, M., Pavlenishvili, E., Schmincke, H.-U., Sologashvili, D., Tushabramishvili, D., Tvalcrelidze, M., Vekua, A., 1989. Der Altpalaolithische Fundplaz Dmanisi in Georgien (Kaukasus). Jahrb. Rom.-Germ. Zentralmus Mainz 36, 67–116.

Farifteh, J., Soeters, R., 1999. Factors underlying piping in the Basilicata region, southern Italy. Geomorphology 26, 239–251.
Ferring, C.R., 1986. Rates of fluvial sedimentation: Implications for archaeological variability. Geoarchaeology 1, 259–274.
Ferring, C.R., 1992. Alluvial pedology and geoarchaeological research. In: Holliday, V.T. (Ed.), Soils in Archaeology, Landscape Evolution and Human Occupation. Smithsonian Institution Press, Washington, pp. 1–39.
Ferring, R., Ohms, O., Agusti, J., Berna, F., Nioradze, M., Shelia, T., Tappen, M., Vekua, A., Zhvania, D., Lordkipanidze, D., 2011. Earliest human occupations at Dmanisi (Georgian Caucasus) dated to 1.85-1.78 Ma. Proc. Natl. Acad. Sci. USA 108, 10432–10436.
Gabunia, L., Vekua, A., 1995. A Plio-Pleistocene hominid from Dmanisi, East Georgia, Caucasus. Nature 373, 509–512.
Gabunia, L., Vekua, A., Lordkipanidze, D., Swisher, C., Ferring, C.R., Justus, A., Nioradze, M., Tvalcrelidze, M., Anton, S., Bosinski, G., Joris, O., de-Lumley, A., Majsuradze, G., Mouskhelishvili, A., 2000. Earliest Pleistocene hominid cranial remains from Dmanisi, Republic of Georgia: Taxonomy, geological setting and age. Science 288, 1019–1025.
Garcia, T., 2004. Cadres stratigraphique, magnetostratigraphique et géochronologique des hominides fossiles du site de Dmanissi en Géorgie. Ph.D. Dissertation, Museum National d'Histoire Naturelle.
Garcia, T., Féraud, G., Falguères, C., de Lumley, H., Perrenoud, C., Lordkipanidze, D., 2010. Earliest human remains in Eurasia: New $^{40}Ar/^{39}Ar$ dating of the Dmanisi hominid-bearing levels, Georgia. Quat. Geol. 5, 443–451.
Gee, G.W., Bauder, J.W., 1986. Particle size analysis. In: Klute, A. (Ed.), Methods of Soil Analysis, Part 1 – Physical and Mineralogical Methods, 2nd ed., Monograph No. 9. American Society of Agronomy, Madison, pp. 383–411.
Gudjabidze, A.E., 2003. Geologic Map of Georgia. Georgian State Department of Geology and National Oil Company 'Saqnavtobi', Tbilisi.
Guillou, H., Carracedo, J.C., Day, S.J., 1998. Dating the Upper Pleistocene Holocene volcanic activity of La Palma using the unspiked K/Ar technique. J. Volcanol. Geotherm. Res. 86, 137–149.
Gutierrez, M., Sancho, C., Benito, G., Sirvent, J., Desir, G., 1997. Quantitative study of piping processes in badlands areas of the Ebro Basin, NE Spain. Geomorphology 20, 237–253.
Halliday, W.R., 2007. Pseudokarst in the 21st century. J. Cave Karst Studies 69, 103–113.
Johnson, D.L., 1989. Subsurface stone lines, stone zones, artifact manuport layers and biomantles produced via pocket gophers (*Thomomys bottae*). Am. Antiq. 54, 370–389.
Johnson, D.L., 1990. Biomantle evolution and the redistribution of earth materials and artifacts. Soil Sci. 149, 84–102.
Jones, J.A.A., Richardson, J.M., Jacob, H.J., 1997. Factors controlling the distribution of piping in Britain: A reconnaissance. Geomorphology 20, 289–306.
Jongmans, A.G., Verburg, P., Nieuwenhuyse, A., van Oort, F., 1995. Allophane, imogolite, and gibbsite in coatings in a Costa Rican Andisol. Geoderma 64, 327–342.
Jöris, O., 2008. Der altpaläolithische Fundplatz Dmanisi (Georgien, Kaukasus). In: Monographien des Römisch-Germanischen Zentralmuseums, Band 74, pp. 37–38.
Lordkipanidze, D., Jashashvili, T., Vekua, A., Ponce de León, M., Zollikofer, C., Rightmire, P., Pontzer, H., Ferring, R., Oms, O., Tappen, M., Bukhsianidze, M., Agusti, J., Kiladze, Kahlke, R., Kiladze, G., Martinez-Navarro, B., Mouskhelishvili, A., Nioradze, M., Rook, L., 2007. Post-cranial evidence from early *Homo* from Dmanisi, Georgia. Nature 449, 305–310.
Lordkipanidze, D., Ponce de León, M., Margvelashvili, A., Rak, Y., Rightmire, G.P., Vekua, A., Zollikofer, C.P.E., 2013. A complete skull from Dmanisi and the evolutionary biology of early *Homo*. Science 342, 326–331.
Lordkipanidze, D., Vekua, A., Ferring, R., Rightmire, P., Agusti, J., Kiladze, G., Mouskhelishvili, A., Nioradze, M., Ponce de León, M., Tappen, M., Zollikofer, C.P.E., 2005. The earliest toothless hominin skull. Nature 434, 717–718.
Lyman, R.L., 1994. Vertebrate Taphonomy. Cambridge University Press, Cambridge.
Mallol, C., 2004. Micromorphological observations from the archaeological sediments of 'Ubeidiya (Israel), Dmanisi (Georgia) and Gran Dolina-TD10 (Spain) for the reconstruction of hominid occupation contexts. Ph.D. Dissertation, Harvard University.
Margvelashvili, A., Tappen, M., Rightmire, G.P., Tsikaridze, N., Lordkipanidze, D., 2022. An ancient cranium from Dmanisi: Evidence for interpersonal violence, disease, and possible predation by carnivores on Early Pleistocene *Homo*. J. Hum. Evol. 166, 1–17.
Messager, E., Lordkipanidze, D., Delhon, C., Ferring, C.R., 2010. Palaeoecological implications of the Lower Pleistocene phytolith record from the Dmanisi Site (Georgia). Palaeogeogr. Palaeoclimatol. Palaeoecol. 288, 1–13.
Messager, E., Nomade, S., Voinchet, P., Ferring, R., Mgeladze, A., Guillou, H., Lordkipanidze, D., 2011. $^{40}Ar/^{39}Ar$ dating and phytolith analysis of the Early Pleistocene sequence of Kvemo-Orozmani (Republic of Georgia): Chronological and paleoecological implications for the hominin site of Dmanisi. Quat. Sci. Rev. 30, 3099–3108.
Mgeladze, A., Lordkipanidze, D., Moncel, M.-H., Despriee, J., Chagelashvili, R., Nioradze, M., Nioradze, G., 2011. Hominin occupations at the Dmanisi site, Georgia, Southern Caucasus: Raw materials and technical behaviours of Europe's first hominins. J. Hum. Evol. 60, 571–596.
Nomade, S., Scao, V., Guillou, H., Messager, E., Mgeladze, A., Voinchet, P., Renne, P.R., Courtin-Nomade, A., Bardintzeff, J.M., Ferring, R., Lordkipanidze, D., 2016. New $^{40}Ar/^{39}Ar$, unspiked K/Ar and geochemical constraints on the Pleistocene magmatism of the Samtskhe-Javakheti highlands (Republic of Georgia). Quat. Int. 395, 45–69.
Pickford, M., 2018. Piping, a geomorphological process relevant to African paleontology and archaeology: Sedimentary, taphonomic and biostratigraphic implications. Comm. Geol. Surv. Namib. 20, 59–86.
Saunders, J.J., Dawson, B.K., 1998. Bone damage patterns produced by extinct hyena *Pachycrocuta brevirostris* (Mammalia: Carnivora), at the Haro River Quarry, northwestern Pakistan. In: Tomida, Y., Flynn, L.J., Jacobs, L.L. (Eds.), Advances in Vertebrate Paleontology and Geochronology, National Science Museum, Monographs No. 14. National Science Museum, Tokyo, pp. 215–242.
Schiffer, M.B., 1983. Toward the identification of formation processes. Am. Antiq. 48, 675–706.
Shelia, T., Ferring, R., Tappen, M., Bukhsianidze, M., Lordkipanidze, D., 2020. Archaeology and formation processes in the M6 Block at Dmanisi. Bull. Georg. Natl. Acad. Sci. 14, 148–152.
Stoopes, G., 2003. Guidelines for the Analysis and Description of Soil and Regolith Thin Sections. Soil Science Society of America, Madison.
Tappen, M., 2009. The wisdom of the aged and out of Africa I. In: Shea, J.J., Lieberman, D.E. (Eds.), Transitions in Prehistory: Essays in Honor of Ofer Bar-Yosef. Oxbow Books for the American School of Prehistoric Research, Oxford, pp. 33–53.
Tappen, M., Ferring, C.R., Lordkipanidze, D., Vekua, A., Kiladze, G., 2002. Preliminary observations on the vertebrate taphonomy of the Dmanisi Locality in the Republic of Georgia. In: de Renzi, M., Alonso, M.V.P., Belichón, M., Pañalver, E., Montoya, P., Márquez-Aliga, A. (Eds.), Current Topics on Taphonomy and Fossilization. Graficas Ronda, S.L., Valencia, pp. 161–170.
Tappen, M., Lordkipanidze, D., Bukshianidze, M., Vekua, A., Ferring, R., 2007. Are you in or out (of Africa)? In: Pickering, T.R., Schick, K., Toth, N. (Eds.), Breathing Life into Fossils: Taphonomic Studies in Honor of C.K. Brain. Stone Age Institute Press, Bloomington, pp. 119–135.
Tejedor, M., Neris, J., Jiménez, C., 2012. Soil properties controlling infiltration in volcanic soils (Tenerife, Spain). Soil Sci. Soc. Am. J. 77, 202–212.
Vekua, A., Lordkipanidze, D., Ferring, C.R., Rightmire, P., Tappen, M., Agusti, J., Nioradze, M., Mushkashvili, A., Ponce de Leon, M., Zollikofer, C., 2005. The earliest toothless hominin skull. Nature 434, 717–718.
Vekua, A., Lordkipanidze, D., Rightmire, P., Agusti, J., Ferring, C.R., Maisuradze, G., Mouskhalisvili, A., Nioradze, M., Ponce de Leon, M., Tappen, M., Tvalcrelidze, M., Zollikofer, C., 2002. A new skull of early *Homo* from Dmanisi, Georgia. Science 297, 85–89.
Verachtert, E., Van Den Eeckhaut, M., Peosen, J., Deckers, J., 2010. Factors controlling the spatial distribution of soil piping erosion on loess-derived soils: A case study from central Belgium. Geomorphology 118, 339–348.
Verachtert, E., Van Den Eeckhaut, M., Martínez-Murillo, J.F., Nadal-Romero, E., Poesen, J., Devoldere, S., Wijnants, N., Deckers, J., 2013. Impact of soil characteristics and land use on pipe erosion in a temperate humid climate: Field studies in Belgium. Geomorphology 192, 1–14.
Welker, F., Ramos-Madrigal, J., Gutenbrunner, P., Mackie, M., Tiwary, S., Jersie-Christensen, R.R., Chiva, C., Dickenson, M.R., Kuhlwilm, M., de Manuel, M., Gelabert, P., Martinón-Torres, M., Margvelashvili, A., Arsuga, J.L., Carbonell, E., Marques-Bonet, T., Penkman, K., Sabidó, E., Cox, J., Olsen, J.V., Lordkipanidze, D., Racimo, F., Laluenza-Fox, C., Bermúdez de Castro, J.M., Willerslev, E., Cappellini, E., 2020. The dental proteome of *Homo antecessor*. Nature 580, 235–238.
White, A.F., Brantley, S.L., 2003. The effect of time on the weathering of silicate minerals: Why do weathering rates differ in the laboratory and field? Chem. Geol. 202, 479–506.
Wood, W.R., Johnson, D.L., 1978. A survey of disturbance processes in archaeological site formation. In: Schiffer, M. (Ed.), Advances in Archaeological Method and Theory. Academic Press, New York, pp. 315–381.
Zack, W., 2013. Geoarchaeological analysis of two new test pits at the Dmanisi Site, Republic of Georgia. M.Sc. Thesis, University of North Texas.
Zehetner, F., Miller, W.P., West, L.T., 2003. Pedogenesis of volcanic ash soils in Andean Ecuador. Soil Sci. Soc. Am. J. 67, 1797–1809.
Zhu, T.X., 1997. Deep-seated, complex tunnel systems – a hydrological study in a semiarid catchment, Loess Plateau, China. Geomorphology 20, 255–267.
Zhu, T.X., 2012. Gully and tunnel erosion in the hilly Loess Plateau region, China. Geomorphology 153–154, 144–155.